JAAS

Accepted Manuscript

This is an *Accepted Manuscript*, which has been through the Royal Society of Chemistry peer review process and has been accepted for publication.

Accepted Manuscripts are published online shortly after acceptance, before technical editing, formatting and proof reading. Using this free service, authors can make their results available to the community, in citable form, before we publish the edited article. We will replace this *Accepted Manuscript* with the edited and formatted *Advance Article* as soon as it is available.

You can find more information about *Accepted Manuscripts* in the Information for Authors.

Please note that technical editing may introduce minor changes to the text and/or graphics, which may alter content. The journal's standard Terms & Conditions and the Ethical guidelines still apply. In no event shall the Royal Society of Chemistry be held responsible for any errors or omissions in this *Accepted Manuscript* or any consequences arising from the use of any information it contains.

ROYAL SOCIETY OF CHEMISTRY

www.rsc.org/jaas

Method for isotope ratio drift correction by internal amplifier signal synchronization in MC-ICPMS transient signals

Alkiviadis Gourgiotis[1], Sylvain Bérail[2], Pascale Louvat[1], Hélène Isnard[3], Julien Moureau[1], Anthony Nonell[3], Gérard Manhès[1], Jean-Louis Birck[1], Jérôme Gaillardet[1], Christophe Pécheyran[2], Frédéric Chartier[4], Olivier F.X. Donard[2]

1. Institut de Physique du Globe de Paris, Sorbonne Paris Cité, Université Paris-Diderot, UMR CNRS 7154, 1 rue Jussieu, 75238 Paris Cedex, France

2. Université de Pau et des Pays de l'Adour, Laboratoire de Chimie Analytique Bio-Inorganique et Environnement/ IPREM UMR 5254, Helioparc Pau Pyrenées 2 Avenue du President Angot, 64053 Pau, Cedex 9, France

3. Commissariat à l'Energie Atomique (CEA), DEN/DPC/SEARS/LANIE, 91191 Gif-sur-Yvette Cedex, France.

4. Commissariat à l'Energie Atomique (CEA), DEN/DPC, 91191 Gif-sur-Yvette Cedex, France.

KEYWORDS

Isotope ratio, signal drift, transient signal, hyphenation, chromatography, laser ablation, amplifier, Faraday, MC-ICPMS, time lag

Abstract

The measurement of isotope ratios by Multi Collection Inductively Coupled Plasma Mass Spectrometry (MC-ICPMS) in transient signals often shows a drift of the isotope signal ratio during signal acquisition. This "isotopic drift" is generally related to the small and distinct time lags between the responses of the amplifiers involved in the Faraday detector configuration. In this work, a method of synchronization of the transient isotope signals for a duration of a few tens of seconds is proposed in order to: 1) quantify the time lags between the amplifiers using the ratios of the raw isotope signals and 2) correct the isotope ratio drifts. The method was successfully tested on lead isotope ratio measurements obtained from two different multi-collector mass spectrometers and setups (flow injection with direct injection and gas chromatography). This approach offered a precise determination of the time lag between the different amplifier systems and an effective correction of the isotope ratio drift. The performances of the methods traditionally used for isotope ratio calculation of transient signals were also compared before and after isotope ratio drift correction.

1 Introduction

Over the past ten years, hyphenated techniques involving Multi Collection Inductively Coupled Plasma Mass Spectrometry (MC-ICPMS) have become a powerful tool in the field of isotope analytical chemistry[1]. Development of on-line coupling methods between the MC-ICPMS and Laser Ablation (LA)[2], High Performance Liquid Chromatography (HPLC)[3], Ion Chromatography (IC)[4], IsoTachoPhoresis (ITP)[5], Gas Chromatography (GC)[6] or Gold Trap (GT)[7], open a new dimension in isotopic analysis in interdisciplinary fields such as earth, life, forensic and nuclear sciences. These hyphenated techniques offer shorter analysis time, higher sample throughput, reduction of cross-contaminations and generally higher sensitivities, relative to off-line techniques. On-line coupling methods provide transient signals with specific time windows generally varying from a few dozen milliseconds to a few minutes, in which the isotope ratios can be accurately measured.

Most experiments reveal a systematic isotope ratio increase or decrease during the transient signal acquisition, also called isotope ratio drift[3, 6, 8-10]. Several hypotheses have been proposed to explain the origin of this drift and the most plausible one is the slow time response of the amplifier system against changes of the input ion signal[3, 11, 12]. This time response depends on the amplifier time constant (also called *tau*, τ), which can vary between the individual collectors, generating a non-uniform response in time of the different Faraday-amplifier systems. Pettke et al.[12] investigated two external *tau* correction schemes and demonstrated that their use significantly minimize the isotope ratio variations in LA-MC-ICPMS transient signals.

Isotope ratio drift during transient signals cannot be corrected for by the most commonly used methods for isotope ratio calculation on transient signals (Linear Regression, Point by Point)[1, 9, 13-16]. Peak Area Integration method[9, 14] is not influenced by the isotope ratio drift due to integration of the total signal, but the important drawback of this method is that it does not provide for the uncertainties of individual isotope ratio measurements.

In this work we present a simple method for the correction of the isotope ratio drift, in transient signals. This method is based on the synchronization of the raw isotope signals and offers a precise calculation of the time lag between the different amplifier responses. This time lag is then used for the isotope ratio drift correction. The feasibility of the method was tested on Pb transient signals obtained by an MC-ICPMS Neptune using flow injection and a demountable direct injection high efficiency nebulizer (d-DIHEN)[17] as the introduction system. The method was then used for Pb isotope ratio drift correction for data acquired with a Nu Plasma MC-ICPMS directly coupled to a Gas Chromatograph. Thirty independent Pb injections were performed and isotope ratio uncertainty, trueness and repeatability of the data before and after isotope ratio drift correction were calculated and compared.

2 Material and methods

2.1 Instrumentation

d-DIHEN - flow injection - *MC-ICPMS (Neptune)*

The Neptune MC-ICPMS (ThermoScientific, Germany) used in this work is housed in the Geochemistry and Cosmochemistry laboratory of the Institut de Physique du Globe de Paris (IPGP). It is equipped with a multi-collector system of nine Faraday cups attached to 10^{11} Ω amplifier resistors (dynamic range from 0 to 50 V). All measurements were performed in static multi-collection mode with Faraday cups. The Faraday-amplifier gains were calibrated daily before the analytical session, yielding a level of reproducibility of the electrical gains better than 10 ppm per day. All amplifiers had been set for compensation of signal decay (*tau* correction) according to the procedure recommended by the manufacturer[18]. For lead isotope ratio measurements, although Hg is not present in the standard solution, intensities at m/z=202 were monitored for possible ^{204}Hg isobaric interference corrections and found to be negligible in the case of this study (<10^{-4} V against ^{204}Pb intensities). All samples were injected into the plasma through a demountable direct injection high efficiency nebulizer[17] (d-DIHEN, Analab, France) directly coupled to a flow injection system. The flow injection system consists of a

six-way high flow valve (FAST, ESI, USA) with an injection loop of 5 µL and a peristaltic pump, which ensures the continuous flow of the carrier solution (HNO_3 0.5M). 5 µL of a 100 ppb SRM981 standard solution were pushed from the carrier solution (HNO_3 0.5M) into the torch, at a rate of 50 µL min^{-1}. Cup configuration for Pb measurements and MC-ICPMS operating conditions are summarized in table 1.

GC - MC-ICPMS (Nu Plasma)

The Nu Plasma HR MC-ICPMS (Nu instrument, Wrexham, U.K.) is housed in the Institute of Analytical and Physicochemical Sciences (IPREM, Pau). It is equipped with twelve Faraday cups attached to 10^{11} Ω amplifier resistors for simultaneous detection (dynamic range from 0 V to 10 V). For Pb isotope ratio measurements, in order to increase the dynamic range of the H4 collector for ^{208}Pb detection, two preamplifiers were connected to the same Faraday cup achieving a 20 V dynamic range (from -10 to 10 V). All measurements were performed in static multi-collection mode with Faraday cups. Amplifier gains were calibrated daily before the analytical session yielding a reproducibility of the electrical gains better than 10 ppm per day. Tau-correction was performed for all Faraday-amplifier systems. Correction for isobaric interference at mass 204 was unnecessary as Hg is not present in the standard solution and because Hg species do not elute at the same time as $PbEt_4$. However, ^{204}Hg presence was monitored using ^{202}Hg and for all injections, ^{202}Hg intensities were below 10^{-4} V. All signals were acquired using the Time Resolved Analysis (TRA) mode with an integration time of 0.5 s. This MC-ICPMS was hyphenated to a Gas Chromatographic system (Focus GC, Thermo Scientific, Milan, Italy) with a commercially available heated transfer line and a double inlet plasma torch[19]. A solution of Tl (NIST SRM997, 200 ng.mL^{-1}) was simultaneously introduced as a wet aerosol through a self-aspirating microconcentric nebulizer (200 µL.min^{-1}) and a cinnabar spray chamber. In this work Tl solution was only used for monitoring instrumental stability over time and not for mass fractionation correction. Cup configuration for Pb measurements and MC-ICPMS operating conditions are summarized in table 1.

2.2 Reagents

All sample dilutions were performed with 0.5 M nitric acid obtained from sub-boiled 14 M nitric acid (EVAPOCLEAN system, Analab, France) and de-ionized water (Milli Q system, Millipore, Milford, MA, USA). The same acid was also used as carrier solution for the flow injection. For all Pb injections (Neptune-dDIHEN and Nu plasma-GC) the standard reference material SRM981 (NIST, USA) was used. All calculations were performed with SRM981 isotope ratio values re-evaluated by Doucelance and Manhès[20] ($^{208}Pb/^{206}Pb$ = 2.1681, $^{207}Pb/^{206}Pb$ = 0.914970(17), $^{204}Pb/^{206}Pb$ = 0.059019(5)). For Tl, the SRM997[21] (NIST, USA) standard solution was used. For GC / MC-ICPMS analysis, the SRM981 was ethylated with $NaBEt_4$ and then injected as $PbEt_4$ in isooctane[19].

2.3 Conceptualization of the isotopic drift in Faraday MC-ICPMS transient signals

Amplifiers time lag and signal ratio drift

As previously mentioned, the time response of the amplifiers depends on the amplifier time constant (τ). The first order time constant of the amplifier system is that of *RC* circuits and $\tau = RC$; where *R* is the feedback resistor (10^{11} Ω) and *C* the dumping capacity (~10^{-12} F) which is used to limit the bandwidth of the amplifier. Typical time constant values of the amplifier systems used in this work are: $\tau \sim (10^{11}\ \Omega) \times (10^{-12}\ \text{F}) \sim 0.1$ s.

The relationship between the input voltage (ion signal) on the *RC* circuit and the output voltage at the input of the electrometer can be described by this equation[22]:

$$\frac{dV_{out}}{dt} = \frac{1}{\tau}\left(V_{in}(t) - V_{out}\right) \quad (1)$$

Where $V_{in}(t)$ and V_{out} are the the *RC* circuit input and output voltages which are functions of time. A simulation of the amplifier *RC* circuit influence on two transient signals (V_a^{in}, V_b^{in}) and on the signal ratio (V_a^{out}/V_b^{out}) for τ_a and τ_b time constants is given in figures 1a and 1b. The input transient signals were simulated using a Log-normal function (2) which is a good approximation of the transient signals presented in this work.

$$V_{in}(t) = h \times Exp\left[-\left(Ln(t/t^{apex})/w \right)^2 \right] (2)$$

Where *h*, t^{apex} and *w*, are parameters corresponding to, amplitude, time of maximum signal and width of the peak respectively. The equation (1) was numerically solved for each signal and for different time constants (τ).

As can be seen in figure 1a, the *RC* circuit output signals (V_a^{out} and V_b^{out}) are slightly shifted to the right relative to the input signals. This shift increases for higher amplifier time constants (slower amplifier time response) and decreases for lower time constants (faster amplifier time response). For identical amplifier time constants ($\Delta\tau = \tau_a - \tau_b = 0$), V_a^{out} time shift is identical to V_b^{out} time shift and no V_a^{out}/V_b^{out} ratio drift is generated (Figure 1b). In case of a time lag between the amplifiers ($\Delta\tau \neq 0$), the time shifts of the output signals are not identical and V_a^{out} and V_b^{out} signals are time shifted relative to each other given by $\Delta t = t_a^{apex} - t_b^{apex}$. Due to this time shift, output signals become enhanced or reduced for a given time relative to what they should be if there was no time shift, generating a V_a^{out}/V_b^{out} signal ratio drift (Figure 1b). This ratio drift increases for higher time shifts and decreases otherwise. Therefore, the time lag between the amplifier responses induces a time shift between the output signals which in turn generates an isotope ratio drift. As the time shift between the output signals is too small to be visualized in figure 1b, a schematic representation is given in figure 1c.

The signal time shift between the output signals (Δt) and the time lag ($\Delta\tau$) between the amplifiers are related, and our simulations showed that for amplifier time constants $\tau \sim 0.1$ s and $\Delta\tau$ varying between 0 and 0.01 s, Δt is identical to $\Delta\tau$ ($\Delta t \equiv \Delta\tau$).

The origin of the amplifier time lag is the slight differences between: 1) the ultrahigh ohmic resistors (ΔR) and 2) the capacities[22] (ΔC). An approximation of the expected time lag range between the amplifiers can be performed using equation 3 (see Supplementary Information SI1).

$$\frac{\Delta\tau}{\tau} = \frac{\Delta C}{C} + \frac{\Delta R}{R} \quad (3)$$

For typical $\Delta R/R$ and $\Delta C/C$ values of the order of 3 % and for τ = 0.1 s, $\Delta\tau$ was found to be ~ 0.006 s. This $\Delta\tau$ value may be smaller in the case of different $\Delta C/C$ and $\Delta R/R$ signs. Identical time constants (τ) can thus be due to identical R and C between the different amplifiers, but also to $\Delta C/C$ = - $\Delta R/R$.

It would be interesting to investigate the evolution of signal ratios during transient signals in a three isotope diagram for different amplifier time lags. For this reason, three transient signals were simulated using equation 2 with signal ratios respecting ^{208}Pb/^{206}Pb and ^{207}Pb/^{206}Pb reference ratio values of the SRM981[20]. Then, equation 1 was numerically solved for the three signals. Time constant of ^{206}Pb signal (τ ^{206}Pb) was fixed at 0.1 s and time constants of ^{208}Pb and ^{207}Pb signals (τ ^{208}Pb, τ ^{207}Pb) varied between 0.097 and 0.013 s ($\Delta\tau$ max of 0.006 s). During the transient signals, for each time constant combination, signal ratios follow a straight line and all lines cross each other in a single point located on the Exponential Mass Fractionation Law (EMFL)[23] (Figure 2). When τ ^{208}Pb = τ ^{207}Pb = τ ^{206}Pb (no time lag), signal ratios are invariant to signal changes and as can be seen in figure 2, all signal ratios take a unique value on the EMFL.

Synchronization of the recorded isotope signals

Considering that the major source of the isotope drift in transient signals is the non-uniform time response of the different amplifiers, our approach is to synchronize the distinct isotopic signals with the signal of one amplifier, which is taken as the reference system. The time lags between the different amplifiers can be calculated by synchronizing the recorded signals as a data treatment ($\Delta t \equiv \Delta \tau$). The synchronization is effective when there is no more drift in the time corrected isotopic signals.

The signal synchronization is illustrated in figure 3 and operates as follows. We consider the transient signals of the isotopes "*a*" and "*b*" measured with two different Faraday-amplifiers. Signal (V_b^{ti}) of "*b*" isotope with its respective timestamp readings per cycle (t_i), as recorded from the onboard computer, is considered as the reference system. The amplifier of the "*a*" isotope lags (slower time response) behind the amplifier of the "*b*" isotope generating a positive signal ratio drift (V_a^{ti} / V_b^{ti}) (Figure 3a).

In order to apply a time correction to the signal of the "*a*" isotope, a function $V_a(t)$ describing the signal time evolution, passing through all points (V_a^{ti}), is needed. To achieve this, the transient signal of "*a*" isotope was modeled using Piecewise Polynomial Interpolation (PPI) (Figure 3b). For this work the PPI was accomplished by using the command "*Interpolation*" of *Mathematica* software. This command numerically interpolates a series of 3rd order polynomial curves through the successive points of the signal thus creating a well-behaving curve (no oscillations that are not supported by the data), rather than to generate a single polynomial. The 3rd order interpolation was chosen because it is the lowest polynomial order for which curvature will be continuous. Each interpolation curve is controlled by ensuring that the Sum of Squared Differences (SSD) between the measured signals (V_a^{ti}) and the calculated values from the function $V_a(t_i)$ signals for each timestamp readings (t_i) are equal to zero.

Determination of the time lag between the amplifiers

We consider the slope (*S*) of the linear regression for the V_a^{ti} / V_b^{ti} isotope ratios (Figure 3a, red line):

$$S = \frac{\sum_{i=1}^{n}\left(\frac{V_a^{ti}}{V_b^{ti}}\right) \times \sum_{i=1}^{n} t_i - n\sum_{i=1}^{n}\left(t_i \frac{V_a^{ti}}{V_b^{ti}}\right)}{\left(\sum_{i=1}^{n} t_i\right)^2 - n\sum_{i=1}^{n} t_i^2} \quad (4)$$

Where *S* is the slope, V_a^{ti} and V_b^{ti} are the blank-corrected intensities per cycle of the "*a*" and "*b*" isotopes respectively (in Volts), t_i is the timestamp reading per cycle (in seconds) as recorded from the onboard computer and *n* is the number of points used for the slope calculation. The *Slope* model (equation 5) can now be easily derived from equation 4 by replacing the measured signals V_a^{ti} by the signal function $V_a(t_i + \Delta t)$. This function gives the intensity of isotope "*a*" at a time slightly before or after t_i (Δt positive or negative).

$$S(\Delta t) = \left| \frac{\sum_{i=1}^{n}\left(\frac{V_a(t_i+\Delta t)}{V_b^{ti}}\right) \times \sum_{i=1}^{n} t_i - n\sum_{i=1}^{n}\left(t_i \frac{V_a(t_i+\Delta t)}{V_b^{ti}}\right)}{\left(\sum_{i=1}^{n} t_i\right)^2 - n\sum_{i=1}^{n} t_i^2} \right| \quad (5)$$

Slope (*S*) is now a function of Δt. Minimization of the *Slope* model calculates the Δt_{min} value for which the slope of the linear regression for V_a^{ti} / V_b^{ti} isotope ratio drift is closest to zero. The absolute value for the slope is used in order to avoid negative slopes during minimization. Δt_{min} represents the time shift (in seconds) between V_a^{ti} and V_b^{ti} signals generated by the time lag ($\Delta\tau$) between the two amplifier systems.

For the V_a^{ti} / V_b^{ti} ratio, Δt_{min} is positive if the amplifier response of the "*a*" isotope is slower than that of isotope "*b*" (reference system) and otherwise negative. Numerical minimizations were performed using the command "*NMinimize"* of the *Mathematica* software.

The Δt_{min} value calculated by the model is then used in equation (6) to correct the isotope ratio drifts:

$$\frac{V_a(t_i + \Delta t_{\min})}{V_b^{ti}} \quad (6)$$

The time shift correction is applied right after data acquisition without any preliminary calibration procedures. This internal correction, implying isotopic ratio signals, offers a precise determination of both the time lags between the Faraday-amplifier signals and the isotopic ratios.

For the amplifier signal synchronization and isotope ratio drift correction, alternative calculations can also be used (see SI3).

3 Results and discussion

3.1 Application to transient signals from d-DIHEN - flow injection - MC-ICPMS

Lead transient signals generated by flow injection connected to a demountable direct injection high efficiency nebulizer (d-DIHEN)[17] were investigated using the Neptune MC-ICPMS. The objective was to obtain an isotope ratio drift due only to the time lag between the amplifier systems. Although the flow injection system has already been used for transient signal studies[8], the use of the d-DIHEN allows an effective elimination of isotope bias caused by memory effects. For this purpose, 100 ppb SRM981 standard solution was pushed through a 5

µL injection loop from the carrier solution (HNO_3 0.5M) into the torch, at a rate of 50 µL min^{-1} and the transient signals were acquired with an integration time (*it)* of 0.5 s.

$^{208}Pb/^{206}Pb$, $^{207}Pb/^{206}Pb$ and $^{204}Pb/^{206}Pb$ isotope ratios were investigated and only $^{207}Pb/^{206}Pb$ ratio showed a significant drift (Figure 4a): Point by Point $^{207}Pb/^{206}Pb$ isotope ratio shows a systematic increase with time over a period of ~30 s. Neptune MC-ICPMS offers the possibility to virtually assign amplifiers to Faraday cups. In a second injection for lead transient signal measurement, amplifiers previously assigned to Faraday cups H1 and H2 were switched. This second measurement shows an inversion of the point by point $^{207}Pb/^{206}Pb$ ratio drift (decrease with time, Figure 4b), and confirms that the amplifiers are the source of the isotope ratio drift. Identical drift range (~0.2%) was observed for both measurements.

For the isotope ratio drift correction, blank-subtracted ^{208}Pb and ^{206}Pb intensities with their respective timestamp readings from the onboard computer were used. Isotope blank intensities of ^{207}Pb and ^{206}Pb isotopes were recorded over ~10 seconds before the transient signal peak. Data processing involves subtracting the 10 s averaged blank from each intensity point for the ^{207}Pb and ^{206}Pb isotopes. ^{206}Pb isotope is used as the reference isotope and timestamp and intensity readings of ^{207}Pb were used to obtain the signal function $V_{207}(t)$ by the PPI method.

In order to efficiently calculate the time shift (Δt_{min}) between H1 and H2 amplifier signals, the *Slope* model was applied over a specific time-zone in which the isotope ratios showed a steady trend, avoiding high isotope ratio noisy or spiky behavior (Figure 4a,b, red line). This zone corresponds to ^{207}Pb intensities higher than ~0.7 V. After *Slope* model minimization (see multimedia files), Δt_{min} values were found to be 0.0031 s and -0.0032 s before and after H1-H2 amplifier switching respectively. From the Δt_{min} signs, it can be concluded that the amplifier assigned to the H2 Faraday cup, before amplifier switching, has a slower time response (higher time constant) relative to H1 amplifier.

Then, the time drift corrected $^{207}Pb/^{206}Pb$ isotope ratios were calculated from equation 6 (Figure 4c,d). Comparing the slope values (*S*) before and after drift correction it is obvious that isotope ratio drifts were effectively corrected (Figure 4a vs 4c and 4b vs 4d).

Using the calculated time shift between the amplifier signals (Δt_{min} = 0.0031 s), it would be possible to reproduce the observed isotope ratio drift and to demonstrate that the ratio drift is generated from the time lag between the amplifiers.

For this purpose, the previously calculated signal function $V_{207}(t)$ was used in order to obtain the $V_{206}(t)$ signal function according to: $V_{206}(t) = V_{207}(t) / 0.920187$. Where 0.920187 is the non-mass fractionation corrected $^{207}Pb/^{206}Pb$ isotope ratio measured in continuous signal mode with an integration time of 4 s (0.920187 ± 80 ppm, 2σ). In this way, the non-time shifted signal functions of the ^{207}Pb and ^{206}Pb isotopes can be obtained. Then, the equation 1 was numerically solved for $V_{207}(t)$ and $V_{206}(t)$ signal functions with time constants τ_{207} = 0.1031 s and τ_{206} = 0.1 s ($\Delta\tau$ = 0.0031 s).

As can be seen in figure 5 the simulated isotope ratio drift is in good agreement with the measured isotope ratio drift. Therefore, we can conclude that the isotope ratio drift is mainly generated by the time lag between the amplifiers and also the time shift between the signals is identical to the time lag of the amplifiers ($\Delta t \equiv \Delta\tau$).

The fact that no drift was observed before amplifier switching for the $^{208}Pb/^{206}Pb$ and $^{204}Pb/^{206}Pb$ ratios is due to nearly identical time constants between the amplifiers involved for these isotope ratio measurements (see SI2). This can be also illustrated in the three isotope diagrams, $^{208}Pb/^{206}Pb$ versus $^{207}Pb/^{206}Pb$. For this diagram, the blank-corrected isotope ratios corresponding to the linear regression zone (Figure 4a, red line zone) were used. Isotope ratios in the $^{208}Pb/^{206}Pb$ vs $^{207}Pb/^{206}Pb$ diagram follow a vertical straight line relative to the x-axis, which crosses the Exponential Mass Fractionation Law (EMFL) (Figure 6a). Based on figure 2, this isotope ratio distribution confirms that $\tau\,^{208}Pb \sim \tau\,^{206}Pb$. Isotope ratio distribution in figure 6 b is more difficult to interpret due to low ^{204}Pb signal favoring high $^{204}Pb/^{206}Pb$ ratio random variations around the EMFL.

After drift correction, the isotope ratios are in much better agreement with the EMFL which proves that amplifier signals had been effectively synchronized (Figure 6c).

3.2 Application to GC-MC-ICPMS for Pb isotope ratios

Isotope ratio drift in GC-MC-ICPMS

The previously developed method for isotope ratio drift correction in transient signals was applied to data acquired by gas chromatography directly coupled to a Nu Instrument MC-ICPMS for Pb isotope ratio determination. These data consist of thirty independent injections of Pb SRM981 standard solution, acquired in static multi-collection mode with an integration time of 0.5 s. Lead elution profiles were reproducible with regards to time, peak-shape and maximum intensity. Typical isotope ratio profiles during Pb elution are given in figure 7. Blank-corrected isotope ratios showed a negative drift for $^{208}Pb/^{206}Pb$ ratio (variation of about 1.05%) and positive drifts for $^{207}Pb/^{206}Pb$ and $^{204}Pb/^{206}Pb$ ratios (variations of about 0.35% and ~0.17%, respectively). Theoretically, when a GC is coupled to an MC-ICPMS, both chromatographic separation and time lag between the amplifiers can be considered as possible sources of the observed isotope ratio drift. Capillary GC column separates species according to their boiling points and thus, isotope fractionation during separation would obey physical laws of isotope mass fractionation favoring the elution of light isotope masses first. Therefore, if the major source of the observed isotope ratio drifts is mass-dependent isotope fractionation in the GC column, $^{208}Pb/^{206}Pb$ and $^{204}Pb/^{206}Pb$ ratios should show positive and negative drifts respectively during Pb elution, which is not what is observed (Figure 7a and c). Only $^{207}Pb/^{206}Pb$ isotope ratio positive drift would be consistent with an isotope mass-dependent fractionation in the GC column (Figure 7b). In figure 8 (blue points), $^{204}Pb/^{206}Pb$ and $^{207}Pb/^{206}Pb$ isotope ratios were plotted against $^{208}Pb/^{206}Pb$ ratios and compared to the Exponential Mass Fractionation Law (EMFL)[23]. For these diagrams, the blank-corrected isotope ratios from the linear regression zones (Figure 7 red line zones) of the thirty injections were plotted together. If the observed drifts had been caused by a mass-dependent fractionation in the GC column, the blue points of figures 8a and 8b should be in good agreement with the EMFL. As can be seen, important deviations from the EMFL clearly point out that the major source of $^{204}Pb/^{206}Pb$, $^{207}Pb/^{206}Pb$ and $^{208}Pb/^{206}Pb$ isotope ratio drifts cannot be the isotope mass-dependent fractionation in the GC column during Pb elution. These deviations are consistent with isotope ratio distributions obtained with a time lag between the amplifiers involved in the Faraday detector configuration ($\tau\,^{208}Pb \neq \tau\,^{207}Pb \neq \tau\,^{206}Pb \neq \tau\,^{204}Pb$,

Figure 2). Therefore, time lags between the amplifiers were considered as the major source of the observed isotope ratio drifts.

GC-MC-ICPMS drift correction

For the isotope ratio drift correction, the same procedure previously described for the d-DIHEN introduction system was used. The ^{206}Pb isotope is considered as the reference system and timestamp and signal readings of ^{204}Pb, ^{207}Pb and ^{208}Pb isotopes were used for obtaining the signal functions $V_{204}(t)$, $V_{207}(t)$ and $V_{208}(t)$ respectively by PPI.

Δt_{min} for ^{208}Pb/^{206}Pb, ^{207}Pb/^{206}Pb and ^{204}Pb/^{206}Pb ratio drifts were calculated using *the Slope* model for each injection (see multimedia files). For both ^{208}Pb/^{206}Pb and ^{207}Pb/^{206}Pb, Δt_{min} were reproducible across the thirty injections, with average values of -0.00706 s (± 2.6%, 2σ) and 0.00269 s (± 8.0%, 2σ) respectively. Δt_{min} values of the ^{204}Pb/^{206}Pb ratio show higher fluctuations between the injections with an average value equal to 0.00115 s (± 74.6%, 2σ) (see SI 4.1). These high fluctuations are probably due to low ^{204}Pb signal which increase the uncertainty of the interpolated ($V_{204}(t)$) data.

It should be noted that, even if the time lag between the amplifiers is the dominant source of the observed isotope ratio drift, mass-dependent isotope fractionation in the GC column cannot be excluded. Isotope fractionation in preparative capillary GC[24], HPLC[25], cryo-GC[26] and ITP[5] separation techniques have already been observed. Column isotope fractionation generates an isotope ratio drift that should be added or subtracted to the drift coming from the amplifiers time lag (addition for the same slope signs and subtraction otherwise). *Slope* model takes into account both processes and therefore in this case Δt_{min} includes the amplifier time lag and eventual column isotope fractionation. Therefore, it should be possible to highlight isotope ratio drift generated by column mass-dependent isotope fractionation by subtracting the amplifier time lag.

To correct measured isotope ratios from the time lag drifts, Δt_{min} values obtained from the *Slope* model were used. When comparing the ^{204}Pb/^{206}Pb, ^{207}Pb/^{206}Pb and ^{208}Pb/^{206}Pb slopes of the linear regressions before and after Δt_{min} correction, it is obvious that isotope ratio drift is efficiently corrected by the model (Figure 7a,b,c) and the corrected isotope ratios are in much better agreement with the EMFL (Figure 7a and b, red points).

For ^{208}Pb intensities higher than 10 V, corrected isotope ratios show a slight deviation from the EMFL. The origin of this deviation has not been identified in this work (see SI 4.2).

Individual injections: uncertainty, repeatability and trueness

The performances of the drift correction on the isotope ratio uncertainty, trueness and repeatability were also tested and evaluated. Data of the thirty independent injections (GC-MC-ICPMS) of the SRM981 standard solution were treated with the methods traditionally used for isotope ratio calculation on transient signals: Point by Point (PbP), Linear Regression (LR) and Peak Area Integration (PAI)[1, 14, 15]. The results of the PbP and LR methods were compared before and after isotope ratio drift correction, whereas for the PAI method only raw data were treated. For the PAI method the integration of 100% of the peak area was selected and therefore the time lag between the amplifiers does not have any importance. Epov et al.[13, 14] found that the best isotope ratio precision using the PAI method was obtained for an integration of 90-95% of the peak area. For our data, two different integration zones of 95% and 100% of the peak area were tested and no significant differences were observed. 100% of the peak zone was used for the LR method[14]. For the PbP method the zone which was used for the *Slope* model was taken into account for isotope ratio calculation (red line segments in Figure 7). For all methods, blank intensities were calculated for each isotope as the average value of a zone (duration ~8 s) before the transient signal peak. The blank contribution was then subtracted from each intensity point of the respective isotopes. Isotope ratio drifts for all injections were corrected using Δt_{min} values obtained from the *Slope* model.

For all methods (PbP, LR, PAI) the instrumental mass fractionation was corrected internally using the $^{208}Pb/^{206}Pb$ ratio of (SRM981)[20] and the exponential mass fractionation law[23, 27] (see SI5).

The blank-corrected $^{207}Pb/^{206}Pb$, $^{204}Pb/^{206}Pb$ ratios (corrected for mass fractionation relative to $^{208}Pb/^{206}Pb$ ratio) were treated by different methods before and after isotope ratio drift correction (Figure 9). Final isotope ratio uncertainty for the PbP and LR methods were calculated for each individual injection by propagating the uncertainties of the mass

fractionation factor ($\beta_{208/206}$) and of the $^{207}Pb/^{206}Pb$, $^{204}Pb/^{206}Pb$ ratios. The latter were calculated as the standard deviations (σ) for the PbP method and as the slope uncertainty (SE) for the LR method. The SE was calculated using the command "*Regress*" of *Mathematica* and can also be calculated using the "*INDEX(LINEST*(…))" function of MS EXCEL[15]. The detailed equation for uncertainty propagation used in this work is given in Supporting Information section 5. Unlike the PbP and LR methods, the PAI method does not provide isotope ratio uncertainty for individual injections. In figure 9, the uncertainty associated with the individual injections for the PAI method was calculated as the repeatability (σ) of the thirty injections. All isotope ratio uncertainties are expressed for a coverage factor k=2. Average values of isotope ratios, individual injection uncertainties, repeatability and trueness are given in table 2.

For the PbP method both individual injection uncertainty and repeatability (σ of thirty injections) of the $^{207}Pb/^{206}Pb$, $^{204}Pb/^{206}Pb$ drift corrected ratios were improved by a factor of 20 and 13 respectively, compared to the results without drift correction. In contrast, for the isotope ratios treated with the LR method, repeatability before and after drift correction seems to be invariant (Figure 9) but individual injection uncertainty was significantly improved by a factor of 14. The improvement of individual injection uncertainty and repeatability after isotope ratio drift correction is more significant for $^{207}Pb/^{206}Pb$ than for $^{204}Pb/^{206}Pb$ ratios, as the time lag Δt_{min} is much larger for this ratio. Drift corrections have no influence on the LR average trueness (trueness of the thirty average measurements). In contrast, for the PbP method drift correction improved average trueness for the $^{207}Pb/^{206}Pb$ ratio and deteriorated it for the $^{204}Pb/^{206}Pb$ ratio (Table 2). However, PbP trueness variations are less than the uncertainty measurements, and are therefore not significant.

For all isotope data a slight but systematic shift from the reference value is observed. The fact that average trueness of PAI, PbP and LR methods (before and after drift correction) are all in good agreement, proves that this shift is not a result of the drift correction model either from the PbP or LR data treatment. This small systematic bias cannot be treated statistically and further investigation is needed in order to identify its origin.

4 Conclusion

In this work we demonstrated that, during transient signal acquisition, the slight time lags between the amplifiers involved in Faraday detector configuration generate an isotope ratio drift. We proposed a method for the internal synchronisation of the raw isotope signals which allowed both the precise determination of the time lags between the amplifiers, and the isotope ratio drift correction. The method was successfully tested for transient signals obtained by d-DIHEN-flow injection-MC-ICPMS and GC-MC-ICPMS. This approach allows the use of the full performance range of the Faraday multi-collectors. The performances of the traditionally used methods for isotope ratio calculation on transient signals were significantly improved after correction of the isotope ratio drifts. The measurement uncertainties were reduced by factors of 20 and 14 for the PbP and LR methods respectively. Repeatability was improved by a factor of 13 for the PbP method and the drift correction benefits were found to be less significant than for the LR method. The method can also be applied to the hyphenation of other sample introduction systems such as LA, HPLC, or IC to MC-ICPMS.

REFERENCES

1. P. Rodriguez-Gonzalez, V. N. Epov, C. Pecheyran, D. Amouroux and O. F. X. Donard, *Mass Spectrometry Reviews*, 2012, **31**, 504-521. DOI: 10.1002/mas.20352.
2. J. Koch and D. Günther, *Applied Spectroscopy*, 2011, **65**, 155A-162A. DOI: 10.1366/11-06255.
3. I. Gunther-Leopold, J. K. Waldis, B. Wernli and Z. Kopajtic, *International Journal of Mass Spectrometry*, 2005, **242**, 197-202.
4. S. Garcia-Ruiz, M. Moldovan and J. I. G. Alonso, *Journal of Chromatography A*, 2007, **1149**, 274-281. DOI: 10.1016/j.chroma.2007.03.048.
5. L. Vio, G. Crétier, F. Chartier, V. Geertsen, A. Gourgiotis, H. Isnard, P. Morin and J.-L. Rocca, *Journal of Analytical Atomic Spectrometry*, 2012, **27**, 850-856.
6. E. A. Krupp and O. F. X. Donard, *International Journal of Mass Spectrometry*, 2005, **242**, 233-242. DOI: 10.1016/j.ijms.2004.11.026.
7. R. D. Evans, H. Hintelmann and P. J. Dillon, *Journal of Analytical Atomic Spectrometry*, 2001, **16**, 1064-1069. DOI: 10.1039/b103247j.
8. I. Gunther-Leopold, B. Wernli, Z. Kopajtic and D. Gunther, *Analytical and Bioanalytical Chemistry*, 2004, **378**, 241-249. DOI: 10.1007/s00216-003-2226-1.
9. M. Dzurko, D. Foucher and H. Hintelmann, *Analytical and Bioanalytical Chemistry*, 2009, **393**, 345-355.
10. E. M. Krupp, C. Pecheyran, S. Meffan-Main and O. F. X. Donard, *Analytical and Bioanalytical Chemistry*, 2004, **378**, 250-255. DOI: 10.1007/s00216-003-2328-9.
11. T. Hirata, Y. Hayano and T. Ohno, *Journal of Analytical Atomic Spectrometry*, 2003, **18**, 1283-1288. DOI: 10.1039/b305127g.
12. T. Pettke, F. Oberli, A. Audetat, U. Wiechert, C. R. Harris and C. A. Heinrich, *Journal of Analytical Atomic Spectrometry*, 2011, **26**, 475-492. DOI: 10.1039/c0ja00140f.
13. V. N. Epov, P. Rodriguez-Gonzalez, J. E. Sonke, E. Tessier, D. Amouroux, L. M. Bourgoin and O. F. X. Donard, *Analytical Chemistry*, 2008, **80**, 3530-3538.
14. V. N. Epov, S. Berail, M. Jimenez-Moreno, V. Perrot, C. Pecheyran, D. Amouroux and O. F. X. Donard, *Analytical Chemistry*, 2010, **82**, 5652-5662. DOI: 10.1021/ac100648f.
15. J. Fietzke, V. Liebetrau, D. Guenther, K. Gurs, K. Hametner, K. Zumholz, T. H. Hansteen and A. Eisenhauer, *Journal of Analytical Atomic Spectrometry*, 2008, **23**, 955-961. DOI: 10.1039/b717706b.
16. S. Kappel, S. F. Boulyga, L. Dorta, D. Günther, B. Hattendorf, D. Koffler, G. Laaha, F. Leisch and T. Prohaska, *Analytical and Bioanalytical Chemistry*, 2013, **405**, 2943-2955. DOI: 10.1007/s00216-012-6674-3.
17. P. Louvat, J. Bouchez and G. Paris, *Geostandards and Geoanalytical Research*, 2011, **35**, 75-88. DOI: 10.1111/j.1751-908X.2010.00057.x.
18. A. Trinquier, C. Bouman and N. L. Schwieters, *Thermo Fisher Scientific, Bremen, Germany*, 2013, **Technical note 30249**.
19. G. Sanabria-Ortega, C. Pécheyran, S. Bérail and O. F. X. Donard, *Analytical Chemistry*, 2012, **84**, 7874-7880. DOI: 10.1021/ac301251b.
20. R. Doucelance and G. Manhès, *Chemical Geology*, 2001, **176**, 361-377. DOI: http://dx.doi.org/10.1016/S0009-2541(00)00409-5.
21. L. P. Dunstan, J. W. Gramlich and I. L. Barnes, *Journal of RESEARCH of the National Bureau of Standards*, 1980, **85**, 1-10.
22. T. Hirata, in *Isotopic Analysis, fundamentals and applications using ICP-MS*, ed. F. Vanhaecke and P. Degryse, Wiley-VCH, Germany. 2012, ch. 4, pp. 93-112.
23. W. A. Russell, D. A. Papanastassiou and T. A. Tombrello, *Geochimica et Cosmochimica Acta*, 1978, **42**, 1075-1090. DOI: http://dx.doi.org/10.1016/0016-7037(78)90105-9.

24. H. Holmstrand, M. Mandalakis, Z. Zencak, Ö. Gustafsson and P. Andersson, *Journal of Chromatography A*, 2006, **1103**, 133-138. DOI: http://dx.doi.org/10.1016/j.chroma.2005.11.009.
25. F. Guéguen, H. Isnard, A. Nonell, G. Stadelmann, M. Aubert and F. Chartier, Goldschmidt 2013 Conference, FLORENCE, ITALY.
26. S. Wehmeier, R. Ellam and J. Feldmann, *Journal of Analytical Atomic Spectrometry*, 2003, **18**, 1001-1007. DOI: 10.1039/b302242k.
27. C. N. Maréchal, P. Télouk and F. Albarède, *Chemical Geology*, 1999, **156**, 251-273. DOI: http://dx.doi.org/10.1016/S0009-2541(98)00191-0.

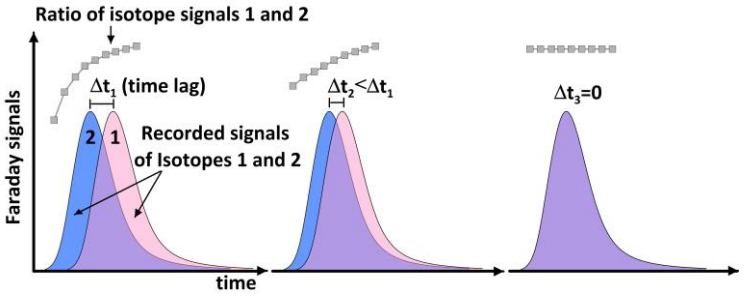

Graphical abstract

MC-ICPMS conditions	Neptune	Nu Plasma
Sample Introduction System		GC
Nebulizer	d-DIHEN	Microconcentric (for Tl)
Spray chamber		Cinnabar 20 mL (for Tl)
Sample gas	0.2 (L min^{-1})	20 (psi)
Ar makeup gas (mL min^{-1})		0.4
He GC carrier gas (mL min^{-1})		25
Liquid uptake (µL min^{-1})	50	200 (for Tl)
MC-ICPMS conditions		
RF power (W)	1200	1300
Plasma gas flow rate (L min^{-1})	15	13
Auxiliary flow rate (L min^{-1})	1.3	0.9
Resolution	Low	Low
Integration time (s)	0.524	0.5 (TRA mode)
Sensitivity on ^{208}Pb (V ppm^{-1}, continuous introduction mode)	120	45

Cup configuration	L3	L2	L1	Ax	H1	H2	H3	H4
Neptune	^{202}Hg		^{204}Pb		^{206}Pb	^{207}Pb	^{208}Pb	
Nu Plasma		^{202}Hg	^{203}Tl	^{204}Pb	^{205}Tl	^{206}Pb	^{207}Pb	^{208}Pb

Focus GC		*GC temp. Program*	
Injector	Split/splitless	Initial temperature (°C)	60
Injector volume (µL)	3	Initial time (min)	2
Injector temperature (°C)	250	Ramp 1 (°C/min)	60
Column	MXT, 30 m, 0.53 mm i.d.,	Final temperature 1 (°C)	95
	1.0 mm coating	Hold time (min)	5
		Ramp 2 (°C/min)	60
		Final temperature 2 (°C)	250
		Hold time (min)	1

Table 1. MC-ICPMS and GC operating conditions and Faraday cup configuration.

$^{207}Pb/^{206}Pb$	**PbP**		**LR**		**PAI**
	Drift uncorrected	Corrected	Drift uncorrected	Corrected	Drift uncorrected
% Uncertainty	0.50	0.024	0.034	0.0024	
% Repeatability	0.098	0.0072	0.0062	0.0062	0.0058
% Trueness	0.030	0.014	0.018	0.019	0.016
$^{204}Pb/^{206}Pb$					
% Uncertainty	0.52	0.088	0.031	0.017	
% Repeatability	0.125	0.034	0.022	0.022	0.062
% Trueness	0.013	0.032	0.030	0.030	0.025

Table 2. Average values of $^{207}Pb/^{206}Pb$ and $^{204}Pb/^{206}Pb$ isotope ratios; uncertainty, repeatability and trueness for data uncorrected and corrected for isotope ratio drift in GC-MC-ICPMS. Where PbP, LR and PAI are respectively the Point by Point, Linear Regression and Peak Area Integration methods. Uncertainty and repeatability are expressed for a coverage factor k=2.

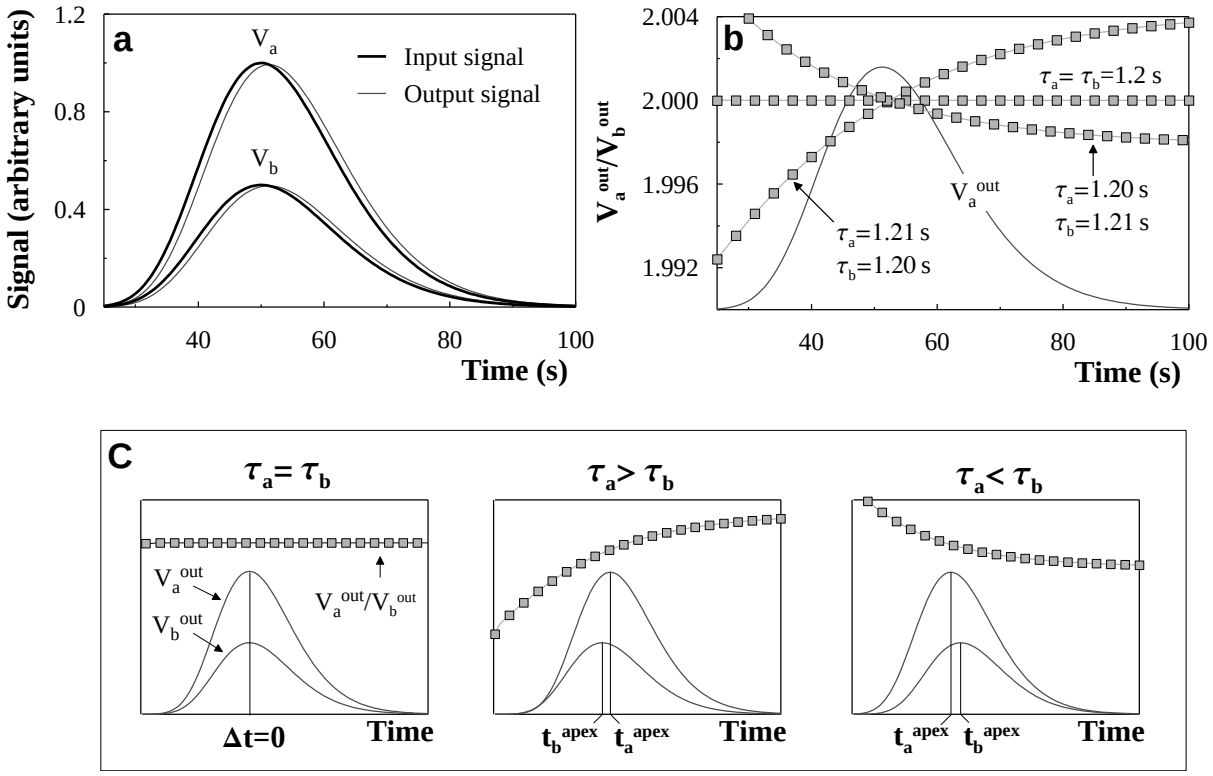

Figure 1. a) Simulation of the amplifier *RC* circuit influence on two input transient signals (V_a^{in} and V_b^{in}). The equation 2 was used for the simulation of the input signals. For both signals, *w* and t^{apex} were equal to 0.4 and 50 respectively and *h* was 1 and 0.5 for V_a^{in} and V_b^{in} respectively. For the resolution of the equation 1, a high time constant was chosen (τ_a = τ_b =1.2 s) in order to better visualize the time shift between the input and the output signals. b) Simulation of the influence of the amplifier time constants (τ_a, τ_b) on the output signal ratios. c) Schematic representation of the time shift between the output signals (typically in the order of some milliseconds) as a function of amplifier time constants.

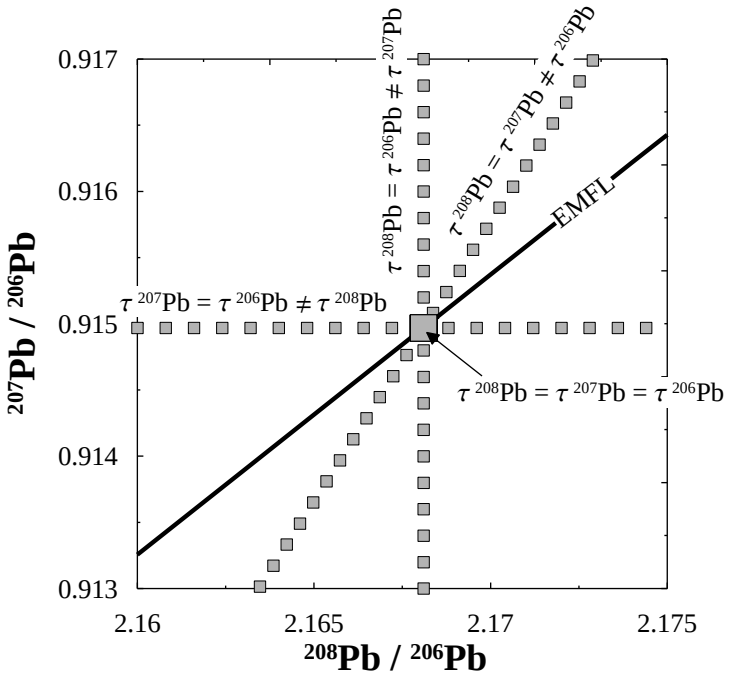

Figure 2. Simulation showing the evolution of signal ratios during transient signals in a three isotope plot for different amplifier time constants. For each time constant combination, signal ratios follow a straight line and all lines cross each other in a single point located on the Exponential Mass Fractionation Law (EMFL). Some particular time constant combinations are presented: $\tau^{208}Pb = \tau^{206}Pb$, $\tau^{207}Pb = \tau^{206}Pb$, $\tau^{208}Pb = \tau^{207}Pb$ and $\tau^{208}Pb = \tau^{207}Pb = \tau^{206}Pb$. For $\tau^{208}Pb = \tau^{207}Pb = \tau^{206}Pb$ (no time lag), signal ratios take a unique value on the EMFL.

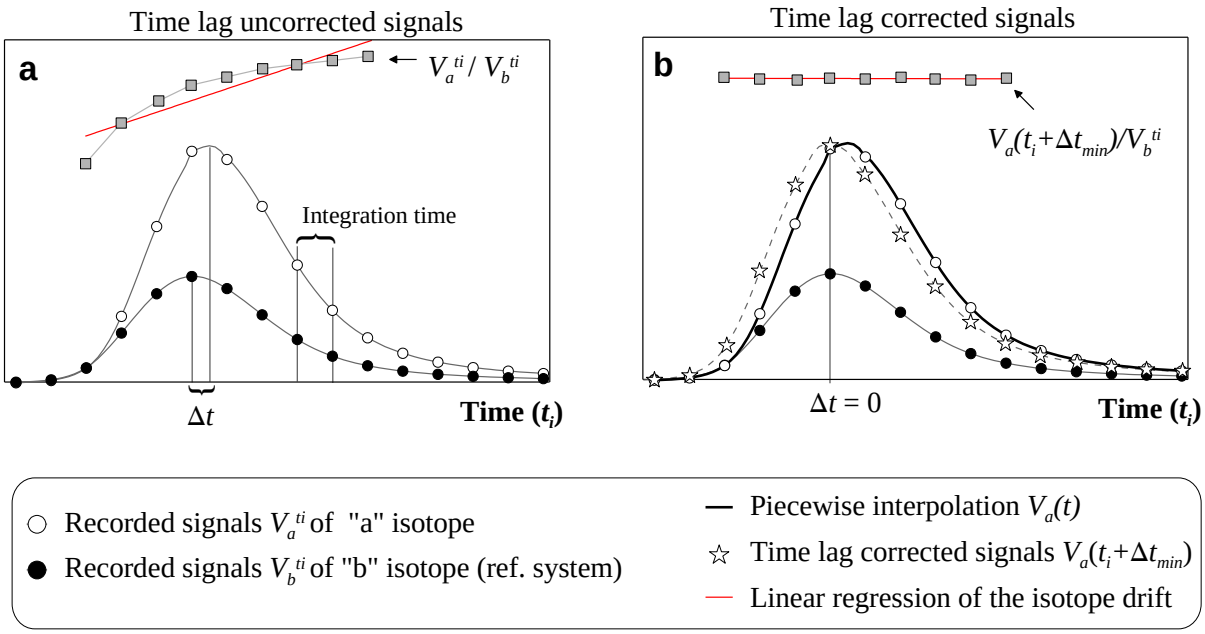

Figure 3. a) A simplified illustration of an exaggerated time shift between two signals for "*a*" and "*b*" isotopes. Considering "*b*" isotope as the reference system, amplifier of the "*a*" isotope lags behind the amplifier of the "b" isotope generating a positive drift in time of V_a^{ti} / V_b^{ti} isotope ratio. Where t_i are the timestamp readings per cycle as recorded from the onboard computer. b) Time lag correction of the "*a*" isotope signals. The time shift value between the signals (Δt_{min}) is calculated by minimizing the slope of the isotope ratio drift. Stars are the new time-corrected signals of the "*a*" isotope which are obtained from the $V_a(t_i+\Delta t_{min})$ function. The drift-corrected isotope ratios are calculated using $V_a(t_i+\Delta t_{min})$ / V_b^{ti}.

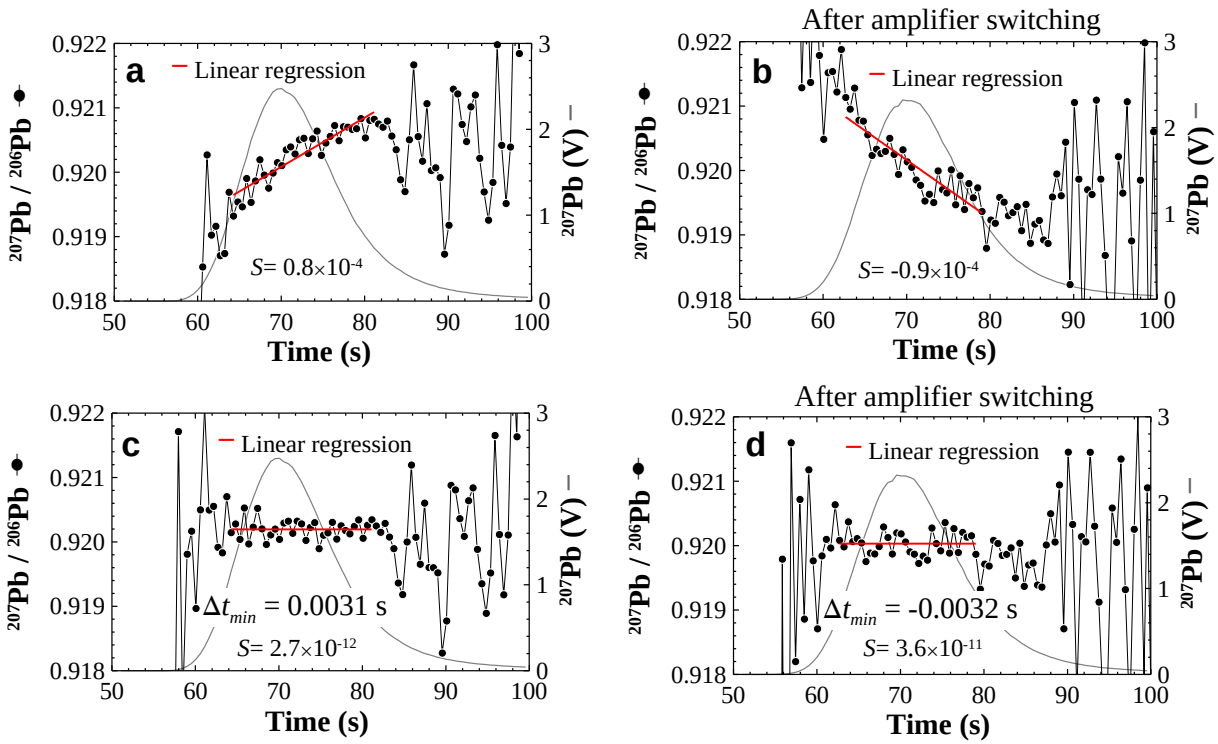

Figure 4. Lead transient signal with flow injection and a demountable direct injection high efficiency nebulizer (d-DIHEN) on a Neptune MC-ICPMS (integration time of 0.524 s). (a) Drift of the point by point isotopic ratio of blank-corrected ^{207}Pb and ^{206}Pb intensities with time. (b) Drift of the point by point isotopic ratio of blank-corrected ^{207}Pb and ^{206}Pb intensities with time after H1 and H2 amplifier switching. (c) and (d) Time lag corrected isotope ratios for (a) and (b) isotope drifts respectively. Red lines correspond to linear regression functions and S to the slope values. Δt_{min} is the value for which the slope is closest to zero and corresponds to the time shift of the ^{207}Pb and ^{206}Pb signals and so to the lag between the amplifiers.

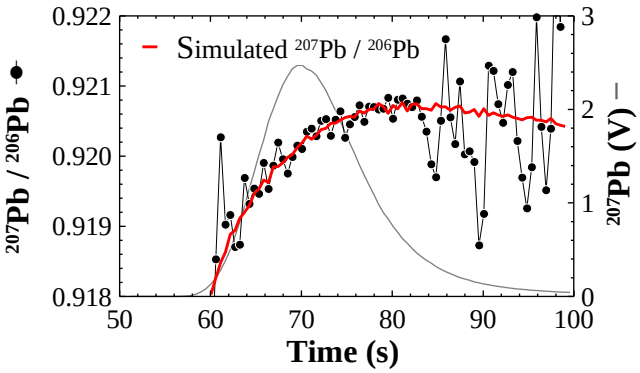

Figure 5. Simulation of the expected $^{207}Pb/^{208}Pb$ isotope ratio drift for lead transient signals with flow injection and a demountable direct injection high efficiency nebulizer (d-DIHEN) on a Neptune MC-ICPMS.

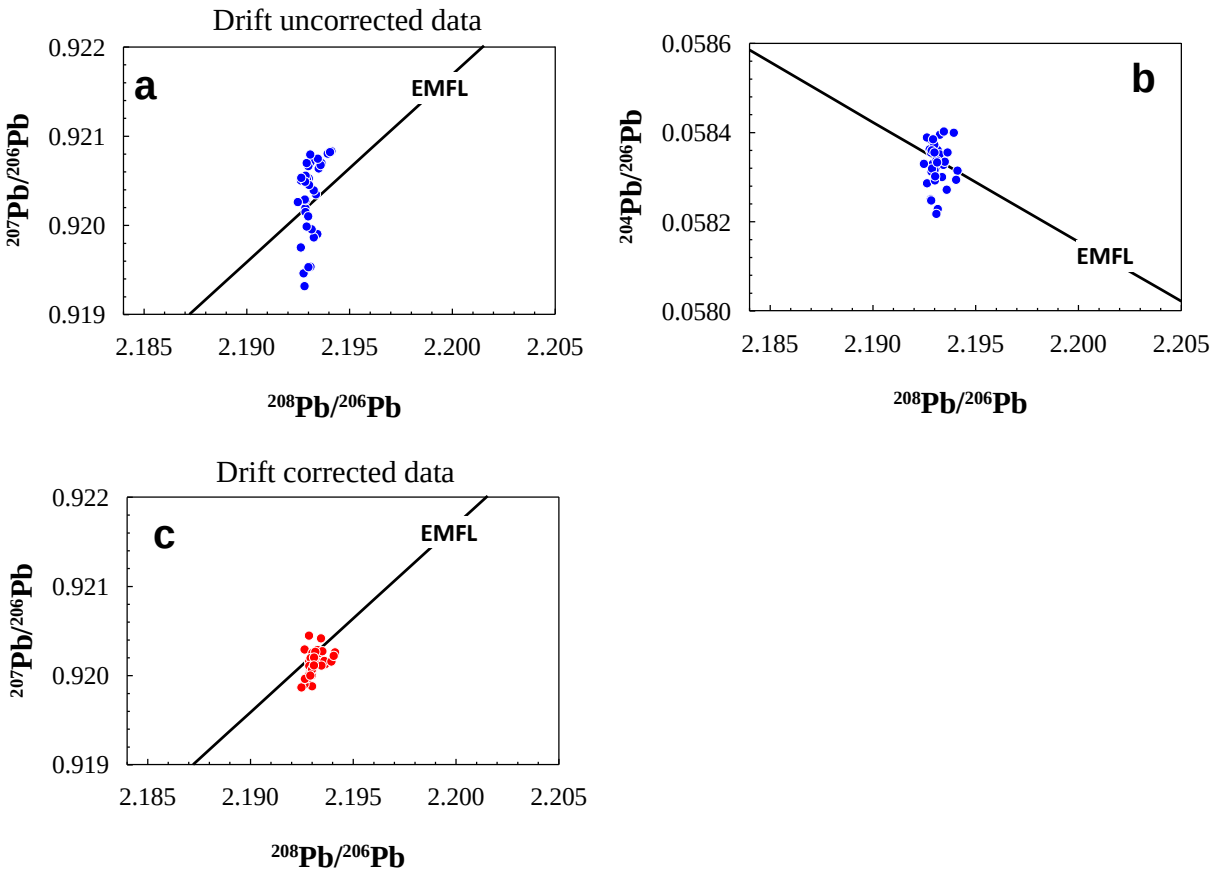

Figure 6. Three isotope plots, for lead transient signals with flow injection and a demountable direct injection high efficiency nebulizer (d-DIHEN) on a Neptune MC-ICPMS. These data were obtained before amplifier H1-H2 switching. Where EMFL, is the Exponential Mass Fractionation Law. a) and b) raw data, and c) drift corrected $^{207}Pb/^{208}Pb$ ratios.

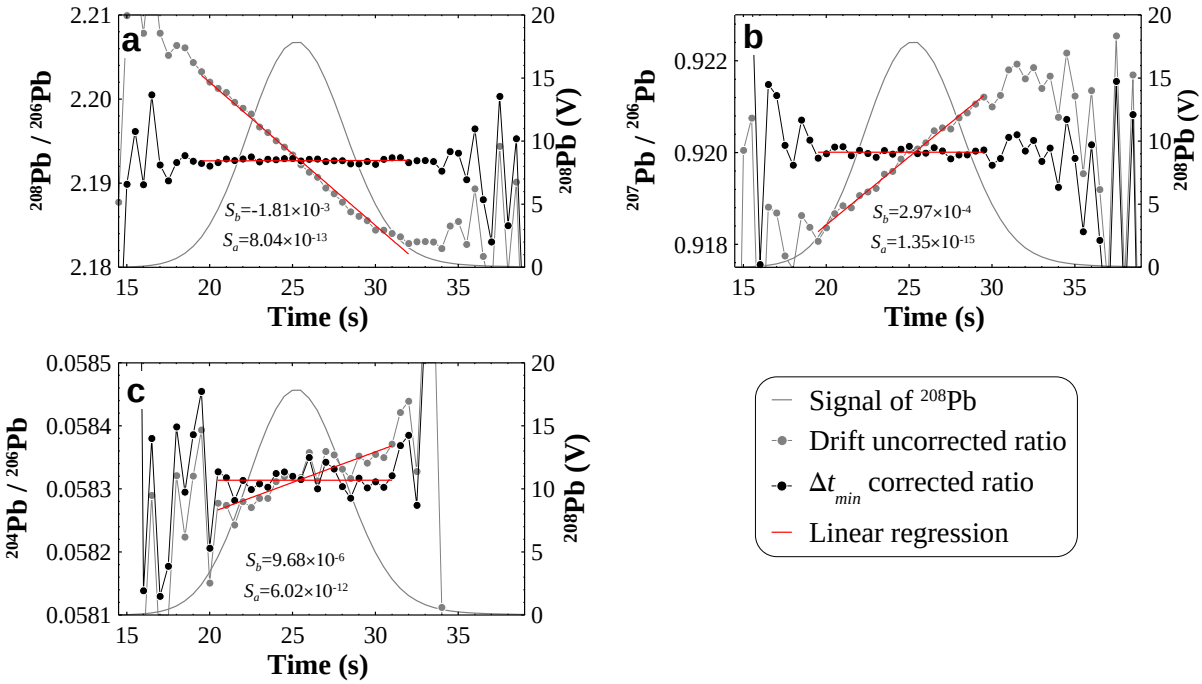

Figure 7. Lead transient signal using a GC directly coupled with a Nu MC-ICPMS. Isotope ratios before and after drift correction of: a) ^{208}Pb/^{206}Pb, b) ^{207}Pb/^{206}Pb and c) ^{204}Pb/^{206}Pb. Red lines correspond to linear regression functions, (S_b) and (S_a) to the slope values before and after isotope ratio drift correction.

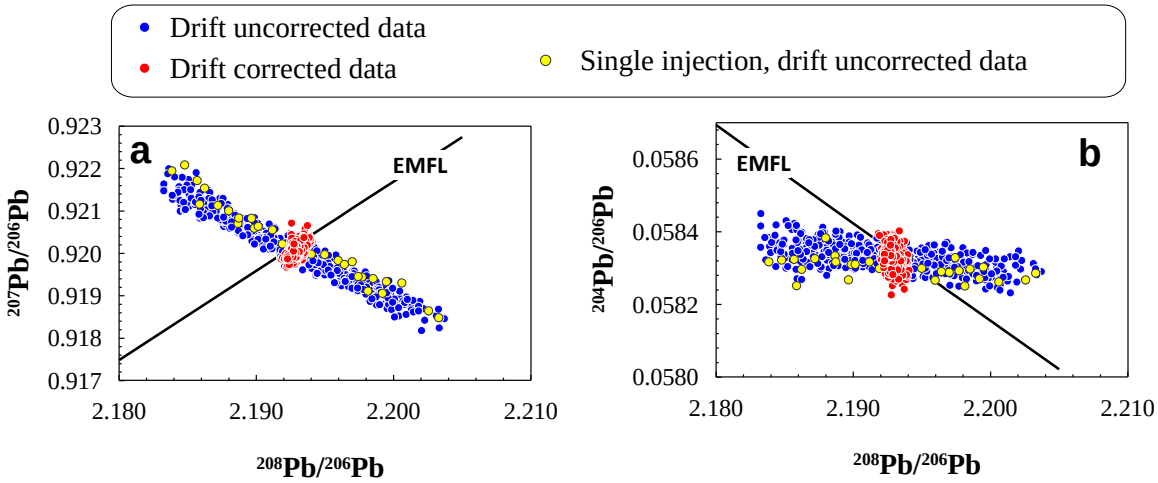

Figure 8. Three isotope plots for lead (SRM981) isotope ratios of 30 independent injections in GC-MC-ICPMS: a) $^{208}Pb/^{206}Pb$ versus $^{207}Pb/^{206}Pb$ and b) $^{208}Pb/^{206}Pb$ versus $^{204}Pb/^{206}Pb$. Blue and red dots represent uncorrected and corrected raw ratios, respectively. Yellow dots show data dispersion characteristic of a single injection. For all lead isotope ratios, the dispersion of the raw ratio points around the Exponential Mass Fractionation Law (EMFL) is much less for corrected compared to uncorrected ratios.

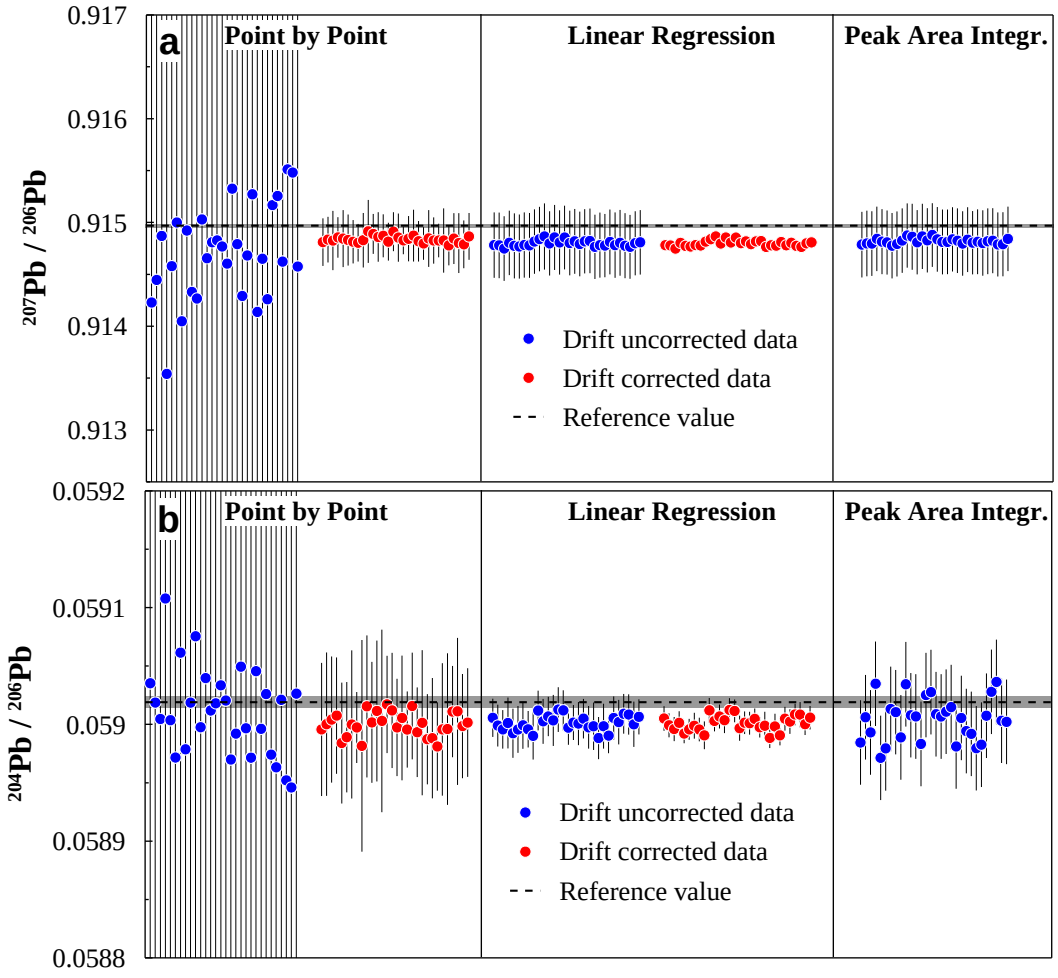

Figure 9. GC-MC-ICPMS blank-corrected and mass fractionation-corrected $^{207}Pb/^{206}Pb$ (a) and $^{204}Pb/^{206}Pb$ (b) isotope ratios for thirty injections. All data were treated before and after isotope ratio drift correction with the Point by Point (PbP), Linear Regression (LR) and Peak Area Integration (PAI) methods. Dashed lines represent reference values of $^{207}Pb/^{206}Pb$ and $^{204}Pb/^{206}Pb$ isotope ratios for the SRM981 standard solution and the shaded areas correspond to the reference value uncertainties (2σ). All uncertainties are expressed for a coverage factor k=2.